CONSTITUTIVE EQUATIONS OF ERYTHROCYTE MEMBRANE INCORPORATING EVOLVING PREFERRED CONFIGURATION

A. TÖZEREN, R. SKALAK, B. FEDORCIW, K. L. P. SUNG, AND S. CHIEN
Bioengineering Institute and Department of Physiology, College of Physicians and Surgeons of Columbia University, New York, New York 10032

ABSTRACT The erythrocyte membrane is modeled as a two-dimensional viscoelastic continuum that evolves under the application of stress. The present analysis of the erythrocyte membrane is motivated by the recent development of knowledge about its molecular structure. The constitutive equations proposed in the present analysis explain in a consistent manner the data on both the deformation and recovery phases of the micropipette experiment. The rheological equations of the present study are applied in a later section to the analysis of a plane membrane deformation that is quantitatively similar to the tank-treading motion of the erythrocytes in a shear field. The computations yield useful information on how the membrane viscosity becomes a more dominant feature in tank-treading motion. The material constants appearing in the proposed constitutive equations may be useful indications of the biochemical state of the membrane in health and disease.

INTRODUCTION

The erythrocyte membrane is modeled as a two-dimensional viscoelastic continuum that evolves under the application of stress. The present analysis of the erythrocyte membrane is motivated by the recent development of knowledge about its molecular structure and by the complex behavior it exhibits in dynamic micropipette testing and in tank-treading during shear flow.

It is well established that the erythrocyte membrane deforms at constant surface area under physiological circumstances (1, 2). The constant area condition is considered to be a reflection of the structure of the lipid bilayer of the membrane. The membrane elasticity exhibited in experiments is primarily due to the network of protein macromolecules embedded in the lipid bilayer. The molecular organization of the entangled protein molecules evolves continuously during a prolonged deformation. The preferred configuration of the membrane from which the elastic strains are measured may not coincide with the initial stress-free configuration. The present model takes into account the evolution of the preferred configuration.

The viscoelastic properties of the erythrocyte membrane were modeled previously by Evans and Hochmuth (3) by using a two-dimensional Kelvin model. Analyzing experimental data with the viscoelastic model of Evans and Hochmuth is simple and useful for obtaining an estimate of the membrane viscosity during rapid deformation. However, the model needs to be further developed to explain the complicated membrane behavior observed in the rapid-transient micropipette experiments of Chien et al. (4). For example, the Kelvin model predicts essentially exponential aspiration length vs. time curves with a single time parameter for both the loading and the recovery phases of the experiment. Chien et al. (4) showed that the deformation of a cell into a micropipette following a step load consists of two phases. The initial rapid phase of deformation has a shear thinning behavior and was modeled recently by Tözeren et al. (5). The rapid phase is followed by a slow deformation phase with high membrane viscosity. The experimental data of Chien et al. (4) also indicate that the time constant of the recovery phase increases with increasing duration of the creep phase for durations of aspiration up to 20 s.

The constitutive equations proposed in the present analysis explain in a consistent manner the data on both the deformation and recovery phases of the micropipette experiment. The rheological equations of the present study are applied in a later section to the analysis of a plane membrane deformation that is quantitatively similar to the tank-treading motion of the erythrocytes in a shear field. The computations yield useful information on how the membrane viscosity becomes a more dominant feature in tank-treading motion. The present constitutive equations have a form similar to that proposed by Evans and Hochmuth (3). However, the membrane viscosity is made to depend on the rate of strain as suggested by Tözeren et al. (5), and the elastic strain tensor is measured from the

Dr. Tözeren's present address is National Institutes of Health, Division of Research Services, Biomedical Engineering and Instrumentation Branch, Bethesda, MD 20205.

evolving preferred configuration. The evolution of the preferred configuration is given by a rate equation. The material constants appearing in the proposed constitutive equations may be useful indications of the biochemical state of the membrane in health and disease. The bending resistance of the membrane is not modeled in the present analysis. The deformation of an erythrocyte membrane during aspiration into a pipette and during tank-treading motion in high-shear flow fields is usually associated with large membrane tensions, and the membrane analysis may be considered to be a sound approximation in such cases.

CONSTITUTIVE EQUATIONS

In this section, the constitutive equations for the erythrocyte membrane are developed in terms of principal strains and stresses. The generalization to the general deformation of a plane membrane is given in the Appendix.

Let the deformation in the membrane be described by initial positions (x_1, x_2) and current positions (y_1, y_2) in a coordinate system tangent to the local principal directions. Extension ratios λ_1 and λ_2 are defined as

$$\lambda_1 = (dy_1/dx_1), \qquad \lambda_2 = (dy_2/dx_2). \tag{1}$$

The surface area of the membrane is assumed to remain constant during deformation. This requires that

$$\lambda_1\lambda_2 = 1. \tag{2}$$

The erythrocyte membrane is composed of a network of protein macromolecules embedded in a lipid bilayer. The network of entangled protein molecules serves as a storage medium for the elastic strain energy in the membrane. The molecular organization of this network evolves continuously during a prolonged deformation. In such cases, the rate of change of the elastic strain may not correspond to the observed rate of deformation.

To measure the elastic strain in the protein network, a two-dimensional symmetric tensor, C_{ij}, is introduced. The diagonal components of this tensor in the principal directions are denoted as I_1^2 and I_2^2, that is:

$$C_{ij} = \begin{bmatrix} I_1^2 & 0 \\ 0 & I_2^2 \end{bmatrix}. \tag{3}$$

At each point of the membrane, the modified stretch ratios I_1 and I_2 define the current geometry relative to the geometry of the preferred configuration through the equations

$$I_1 = dy_1/dz_1, \qquad I_2 = dy_2/dz_2 \tag{4}$$

where (dy_1, dy_2) and (dz_1, dz_2) are the infinitesimal length elements in the current and preferred configurations, respectively. The preferred configuration describes the thermodynamic state of the protein network in which the elastic strains are zero. The degree of evolution of the preferred configuration is measured by the stretch ratios q_1 and q_2, which are defined as

$$q_1 = (dz_1/dx_1) = \lambda_1/I_1 \tag{5a}$$

$$q_2 = (dz_2/dx_2) = \lambda_2/I_2. \tag{5b}$$

In the present deformation the internal elastic strains are assumed to be area preserving, i.e.,

$$I_1I_2 = 1, \qquad q_1q_2 = 1. \tag{6}$$

The viscoelastic model of Evans and Hochmuth (3) is modified as the basis of the constitutive equations developed in this section. The principal membrane tensions T_1 and T_2, which have the units of force per unit length, are assumed to be of the form

$$T_1 = T_0 + 2\eta(\dot{\lambda}_1/\lambda_1) + \mu(I_1^2 - I_1^{-2}) \tag{7a}$$

$$T_2 = T_0 + 2\eta(\dot{\lambda}_2/\lambda_2) + \mu(I_2^2 - I_2^{-2}) \tag{7b}$$

where T_0 is an isotropic tension due to the constant area stipulation, and η and μ are the coefficients of viscosity and elasticity, respectively. The symbol, $\dot{\lambda}_1$, denotes the material time derivative of λ_1. The quantity, $(\dot{\lambda}_1/\lambda_1)$, is the rate of strain in the x_1 direction, and $(\dot{\lambda}_1/\lambda_1) = -(\dot{\lambda}_2/\lambda_2)$ due to the constant area condition (Eq. 2).

To incorporate the shear thinning behavior of the membrane into Eq. (7), the following relation proposed by Tözeren et al. (5) is adopted:

$$\eta = \mu\{\tau^*/[1 + \tau'(\dot{\lambda}_1/\lambda_1)]\} \tag{8}$$

where τ^* and τ' are constants having the dimensions of time.

The time rate of change for the membrane's preferred configuration is assumed to depend on the elastic tension, $T_1^e = \mu(I_1^2 - I_1^{-2})$, through the expression

$$\mu(I_1^2 - I_1^{-2}) = \eta_1(\dot{q}_1/q_1) + \mu_1(q^2{}_1 - q_1^{-2}) \tag{9}$$

where η_1 and μ_1 are constant parameters. The set of constitutive equations proposed for the erythrocyte membrane in the present study is composed of Eqs. 7, 8, and 9. The membrane is considered to be in the preferred configuration when the elastic stretch ratios I_1, I_2 are equal to unity at any point in the membrane. The viscosity coefficients η_1 and η appearing in the constitutive equations may be considered to be measures of the viscous resistance between the entangled protein macromolecules with each other and with the lipid bilayer, respectively. The elasticity coefficient μ is a measure of the elastic properties of the protein network. The dimensionless ratio $b = (\mu_1/\mu)$ indicates the capacity of the network to evolve under stress. As $b \to \infty$, the preferred configuration of the membrane will always remain the same even during sustained deformation; on the other hand, the proposed constitutive equations will describe an elastic liquid membrane with fading memory if the evolution parameter $b = (\mu_1/\mu)$ is set equal to zero.

For sufficiently small deformations, the proposed constitutive equations can be linearized. After eliminating the internal variable I_1 from Eqs. 7, 8, and 9, the following single differential equation is obtained:

$$(T_1 - T_0)[1 + (\mu_1/\mu)] + (\eta_1/\mu)(\dot{T}_1 - \dot{T}_0) = 2\mu\epsilon + 2(\eta + \eta_1)\dot{\epsilon} + 2[\eta_1(\eta/\mu)]\ddot{\epsilon} \tag{10}$$

where $\epsilon = (1/2)(\lambda_1^2 - 1)$ is the strain in the x_1 direction. When ϵ is sufficiently small, the differential equation can be represented by a one-dimensional mechanical analog of a four-parameter solid as shown in Fig. 1 *a*. If the parameter $b = (\mu_1/\mu)$ is set equal to zero, the constitutive equations in the linearized form become identical to those of Jeffrey's fluid model, Fig. 1 *b*, written in two dimensions (6). The nonlinear constitutive equations of the Maxwell type that were developed by Evans and Skalak (7) can be obtained from Eqs. 6 and 8 as a special case by setting the parameters η and μ_1 equal to zero. A phenomenological theory similar to Jeffrey's fluid model with fading memory for polymeric fluids was proposed recently by Dashner and Vanarsdale (8). The protein macromolecules in solution are much more mobile and fluid than the corresponding network embedded in a membrane. The erythrocyte membrane has a more nearly solid-like behavior. The constitutive equations proposed in the present study may also be applicable to other biological membranes with similar molecular structures.

APPLICATION TO MICROPIPETTE EXPERIMENTS

Consider an infinite plane membrane that is aspired into a pipette of radius R_p (Fig. 2). Let R', ϕ', Z' be the dimensional cylindrical

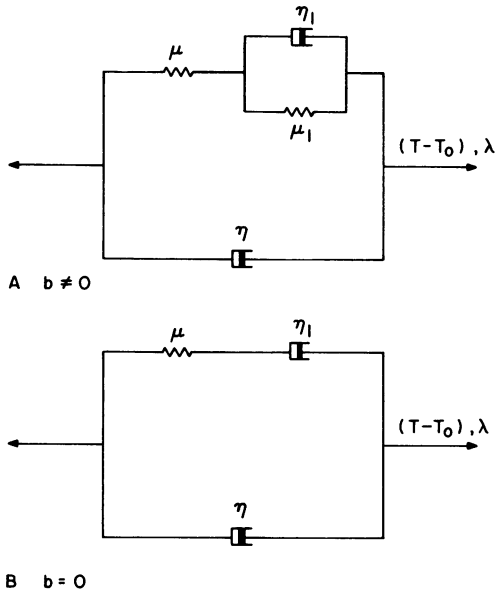

FIGURE 1 The one-dimensional linearized mechanical analogue of the proposed constitutive theory.

coordinates and set $R = R'/R_p$, $Z = Z'/R_p$. The dimensionless coordinates (R_0, ϕ_0, Z_0) and (R, ϕ, Z) are used to denote, respectively, the initial and deformed coordinates of the same material point in the membrane.

The time-dependent deformation of the membrane outside the pipette is described by

$$R^2 = R_0^2 - A(t) + 1, \qquad R \geq 1 \tag{11}$$

where $(\pi R_p^2 A)$ denotes the surface area of the membrane inside the pipette. The extension ratio λ_1 and the rate of strain $(\dot{\lambda}_1/\lambda_1)$ corresponding to the deformation given by Eq. 11 can be expressed as

$$\lambda_1^2 = (dR/dR_0)^2 = R_0^2/[R_0^2 - A(t) + 1] \tag{12a}$$

$$(\dot{\lambda}_1/\lambda_1) = \dot{A}(t)/\{2[R_0^2 - A(t) + 1]\} \tag{12b}$$

It is assumed that the portion of the membrane inside the pipette is parallel to the pipette wall at the exit. Then the mechanical equilibrium of the membrane in the direction of the axis of the pipette requires that

$$(2T_p/\mu) = (\Delta p R_p/\mu) \tag{13}$$

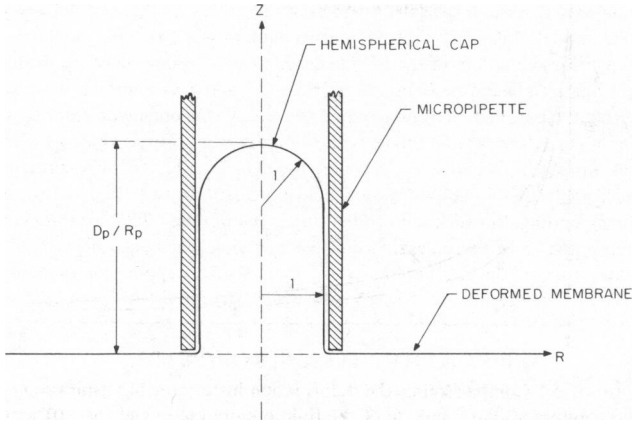

FIGURE 2 Schematic diagram of membrane and aspiration.

where T_p is the meridional tension at the tip of the pipette, and Δp is the applied pressure difference. The membrane tensions T_1 and T_2 are assumed to be continuous at the tip of the pipette. Eq. 13 is valid in the absence of substantial frictional forces and glass adhesion. The effect of adhesive forces will be discussed in the next section.

The static equilibrium in the radial direction of the planar portion of the membrane can be shown to require the following condition:

$$(T_p/\mu) = \int_1^\infty (T_1 - T_2)\, dR/R \tag{14}$$

where T_1 and T_2 denote the radial and circumferential tensions, respectively. Eq. 13 can be used to replace (T_p/μ) in Eq. 14 in terms of the dimensionless tension $(\Delta p\, R_p/\mu)$. Eqs. 12a and 12b, specifying λ and $\dot{\lambda}$ in terms of aspiration history $A(t)$, are then substituted into the constitutive Eqs. 7 and 8 to evaluate $(T_1 - T_2)$ in Eq. 14. After some manipulation, an equation governing micropipette aspiration is obtained in the following form:

$$(\Delta p R_p/\mu) = (2/\alpha) \ln (1 + \alpha\tau^* \dot{A}) + \int_1^\infty (l_1^2 - l_1^{-2})\, (dR/R^2) \tag{15}$$

where $\alpha = \tau'/(2\tau^*)$. The time rate of change of the elastic extension ratio l_1 is governed by the rate equation (see Eq. 9):

$$l_1^2 - l_1^{-2} = 4a\tau^*\left(\frac{\dot{\lambda}_1}{\lambda_1} - \frac{\dot{l}_1}{l_1}\right) + b\left(\frac{\lambda_1^2}{l_1^2} - \frac{l_1^2}{\lambda_1^2}\right) \tag{16}$$

where the coefficients a and b are defined as

$$a = (\eta_1/\mu\tau^*), \qquad b = (\mu_1/\mu). \tag{17}$$

The material time derivative $\dot{l}_1$ is defined as the time derivative of l_1 with R_0 kept constant. Eq. 16 is obtained by using Relations 2 and 5 in Eq. 9.

Eqs. 11, 12, 15, and 16 comprise a set of nonlinear integro-differential equations to be solved simultaneously. For a given case of membrane aspiration, it is assumed that R_p, τ^*, τ', μ, μ_1, a, b, α, and the applied pressure Δp are known values. Eqs. 11, 12, 15, and 16 are to be solved for A as a function of t, and R, λ_1, l_1 as functions of R_0 and t. The stretch ratio λ_1 and the elastic stretch ratio l_1 must be specified as initial conditions. For the deformation phase (the aspiration into the pipette under the application of pressure difference Δp), the initial conditions may be taken to be

$$\lambda_1 = 1, l_1 = 1 \qquad \text{at } t = 0. \tag{18}$$

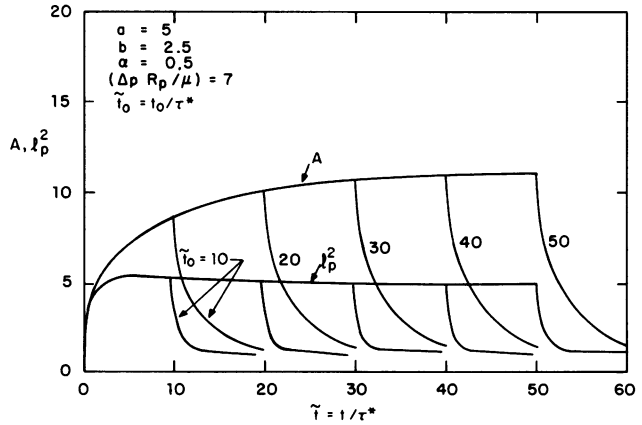

FIGURE 3 Dimensionless surface area A $(A \simeq 2D_p/R_p)$ and elastic strain l_p^2 at the tip of the pipette as a function of dimensionless time $\tilde{t}$ $(\tilde{t} = t/\tau^*)$.

The set of Eqs. 11, 15, and 16 is solved numerically by using a finite difference scheme in time. The value $\dot{A}$ is obtained at each time step from Eq. 15. Then Eq. 12 is used to compute λ_1 and $\dot{\lambda}_1$. Next, Eq. 16 is used to calculate $\dot{l}_1$ as a function of the radial distance R_0 and t. The values of $\dot{l}_1$ and $\dot{A}$ together with the values of A and $\dot{l}_1$ at the kth time step are used to estimate the values of A and l at the $(k + 1)$th time step by using the first two terms of the Taylor's series expansion. This iterative procedure is continued until the end of the deformation phase. The recovery phase is computed in a similar manner, setting $(\Delta p R_p/\mu)$ equal to zero in Eq. 15.

NUMERICAL RESULTS

The time history of deformation of the membrane has been computed for the recovery and creep phases of the micropipette experiment. Fig. 3 shows the dimensionless surface area inside the pipette, A, as a function of the dimensionless time, $\tilde{t} = (t/\tau^*)$, during the creep and recovery phases using constants $b = 2.5$, $\alpha = 0.5$, and $a = 5$. Various recovery curves are shown in the figure as a function of the duration of the creep phase, t_0. The dimensionless applied pressure difference $(\Delta p R_p/\mu)$ was taken to be $(\Delta p R_p/\mu) = 7$. The time rate of change of A, $\dot{A}$, approaches zero as the dimensionless duration of the creep phase, $\tilde{t}_0 = t_0/\tau^*$ increases. A finite b value always has a steady state equilibrium at $t = \infty$. Similarly, $\dot{A}$ approaches zero in the recovery phase as the equilibrium length (D_p/R_p) decreases to zero.

The dimensionless surface area A inside the pipette is equal to λ_p^2, the square of the extension ratio λ at the tip of the pipette, and was previously considered to be a measure of the elastic strain (3, 4). This is correct for short periods of deformation, measured in milliseconds. The present model takes into account the rearrangement of the protein network in the membrane during longer periods of deformation. Fig. 3 shows the variation of the elastic stretch ratio, $l_1^2 = l_p^2$, at the tip of the pipette with respect to time during the creep and recovery phases. The stretch ratio l_1/l_1 is a function of time and position $[l_1 = l_1(R, t)]$. The functional dependence of l_1 on the radius R is quite similar to the corresponding relation $\lambda_1 = \lambda_1(R, t)$ at the initial stages of the creep phase. However, as the duration of the numerical experiment increases, this functional relation holds only in the region $R > M$, where M is sufficiently large. Fig. 4 illustrates l_1 at steady state as a function of distance R.

The value of b is important in the determination of the membrane behavior after long periods of deformation. If the constant b is set equal to zero, the membrane has the properties of a fluid. The time histories of aspiration area $A = A(t)$ are compared in Fig. 5 for two membrane models with $a = 10, b = 2$ and $a = 10, b = 0$. The figure shows that there is very little difference between these models in the initial phase of deformation. However, the membrane model with $b = 2$ approaches steady state as the duration of the creep phase, $\tilde{t}_0$, increases. On the other hand, in the case of a fluid membrane ($b = 0$), the aspiration area A increases linearly with t (constant $\dot{A}$) for large $\tilde{t}_0$. The membrane model with a finite b value recovers its initial

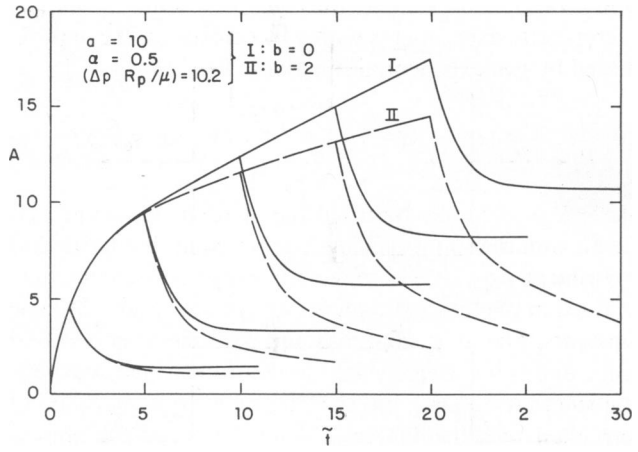

FIGURE 4 The variation of the elastic stretch ratio ℓ as a function of the dimensionless radius R at steady state ($t = \infty$).

state at the end of the relaxation process. In contrast, there is a permanent deformation at the end of the recovery in the case of the fluid membrane as illustrated in Fig. 5. The data presented by Chien et al. (4) on the partial aspiration of red blood cells in a pipette indicate that a steady state deformation is reached in <1 min during the creep phase and that the red blood cell recovers its initial shape shortly after the pressure difference Δp is set equal to zero. The analysis of the membrane model with a finite b value produces results that are consistent with this experimental observation. The protein matrix lining the red cell membrane is connected to the protein molecules spanning the lipid bilayer (9). It is expected that the rearrangement of the network of the protein molecules will be restricted to some extent, leading to the possibility of a finite b value.

To estimate the parameters a and b appearing in the rate Eq. 16, various time constants observed in micropipette experiments must be considered. The greater part of the deformation into the pipette occurs during the initial rapid phase. Chien et al. (4) showed that the experimental

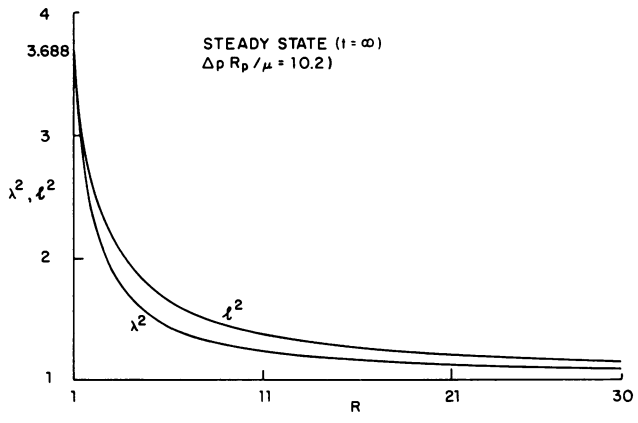

FIGURE 5 Comparison of the deformation history during aspiration of the membrane into a pipette of the fluid membrane model ($b = 0$) with that of the solid membrane model ($b = 2$).

aspiration length history during the loading phase of micropipette experiments on red blood cells can be approximated by two exponential functions of the form

$$\frac{D_p}{R_p} = \frac{D'_{pm}}{R_p}(1 - e^{-t/\beta_1}) + \left(\frac{D_{pm}}{R_p} - \frac{D'_{pm}}{R_p}\right)(1 - e^{-t/\beta_2}) \quad (19)$$

where R_p is the inner radius at the tip of the pipette, D_{pm} is the maximum aspiration length achieved in that particular experiment, D_{pm}', is the apparent steady state deformation attained in the first rapid phase, and β_1 and β_2 are the time constants. The short time constant, β_1, varies over a sixfold range and is inversely related to the dimensionless aspiration length (D'_{pm}/R_p), but the long time constant, β_2, is not correlated with the degree of deformation. In the present model, D'_{pm} is defined as the aspiration length where the difference between the extension ratio λ and the elastic stretch ratio l_1 reaches a certain magnitude, i.e., when $(\lambda_1^2 - l_1^2)/\lambda_1^2 = 0.05$ at the tip of the pipette. The aspiration length D_p/R_p (Fig. 2) is assumed to be related to the surface area of the aspiration by the following relation:

$$A = 2\,D_p/R_p, \qquad D_p/R_p \geq 1. \quad (20)$$

In the derivation of Relation 20, it is assumed that the aspirated portion consists of a hemispherical cap with radius R_p connected to a cylinder with radius R_p and length $(D_p - R_p)$ (4). If the generalized Kelvin model proposed by Evans and Hochmuth (3) is used in the analysis of the deformation phase of the micropipette experiments, the theoretically predicted time parameter β_1 turns out to have a constant value and β_2 becomes equal to zero. However, the shear thinning behavior during the rapid phase of cell deformation into the pipette (the decrease in the value of β_1 with increase in either D_{pm}/R_p or $\Delta pR_p/\mu$) is described accurately with the present model, since this model is the extension of the constitutive equations of Tözeren et al. (5) into the range of long periods of deformation.

Fig. 6 shows the time constant β_1 predicted by the present theory and the experimental results of Chien et al. (4) as a function of the dimensionless aspiration ratio (D_{pm}/R_p) at steady state.

The recovery phase in the micropipette is initiated when the aspiration pressure Δp is removed, and the aspirated portion of the red blood cell relaxes inside the pipette. Experiments showed that the recovery curve could be approximated by an exponential curve with time constant β_r and that β_r was approximately equal to the time constant, β_1, of the rapid phase of deformation if the duration of deformation, t_0, was short ($t_0 < 2$ s). The time constant β_r increased with the duration t_0 until a steady state was reached. It was observed that the β_r values obtained after a 20 s deformation period did not show a dependence on the degree of the deformation and were approximately equal to the time constant β_1 observed for small ($\Delta pR_p/\mu$) values in the deformation phase of the experiment. The computations with the present model also indicate that the time constant β_r is equal to the short time constant, β_1, of the loading phase for short durations, and that it increases gradually with the duration of deformation. The value of $\dot{A}$ at the initiation of the recovery phase is not sensitive to the duration of the deformation phase, and is approximately equal to the value of $\dot{A}$ at the start of the slow deformation phase for the case of perfect slip between the membrane and the pipette. Hence, the increase in the value of β_r with the duration of deformation is due to the increase of A with time for a given dimensionless tension ($\Delta pR_p/\mu$). To obtain numerical results compatible with experimental observation on recovery time

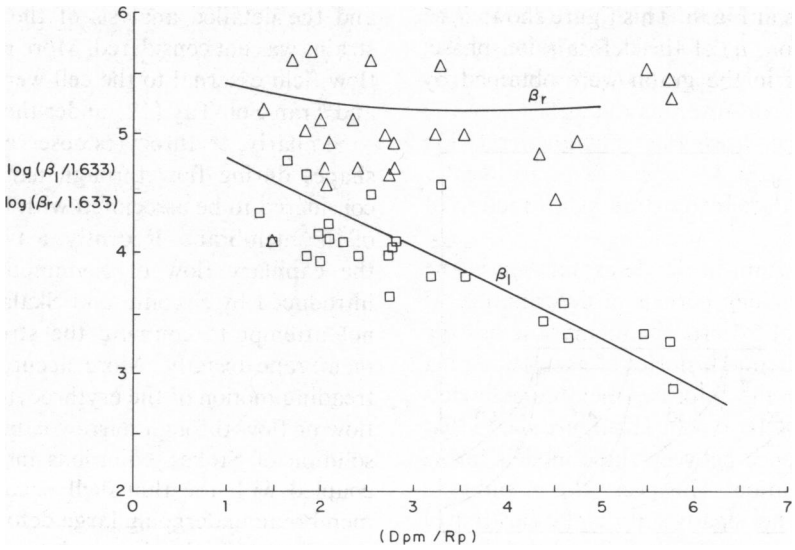

FIGURE 6 Variations of the time constants β_1 and β_r as functions of dimensionless maximum aspiration length (D_{pm}/R_p). The discrete points are the experimental values presented by Chien et al. (4) (□: deformation phase; △: recovery phase). The continuous curves are the predictions of the present model ($b = 1.5$, $a = 50$).

constant variation, the value of b must be taken in the range ($0 \leq b \leq 0.6$), but this leads to large values of the ratio (D_{pm}/D'_{pm}) which are inconsistent with experimental results. This result suggests the possibility of adhesive forces between the pipette and the membrane.

Although the experimental data showed a steady state deformation and complete recovery, a two-dimensional fluid model for the red blood cell membrane cannot be excluded categorically. In such a fluid model, the steady state behavior observed in experiments could result from adhesive forces arising between the pipette and the membrane during the course of the deformation. The lack of a permanent deformation at the end of the recovery phase might be attributed, in such a fluid model, to the elastic bending energy of the membrane which is not taken into account in the analysis.

The development of adhesive forces is expected with increasing duration of the loading phase. In the discussion below, the limiting case at the other extreme of the perfect slip condition, namely the perfect adhesion condition, is considered after a certain time t_a, e.g., 2 s. In this case, λ in Eq. 16 is set equal to zero from t_a to the beginning of the computations of the recovery phase. Fig. 7 shows the results for deformation and recovery history of a numerical experiment computed on this basis. The rate of recovery decreases with the duration of the aspiration phase, $\tilde{t}_0$. This causes the time constant β_r to increase with $\tilde{t}_0$. The maximum value of β_r/β_1 depends strongly on the value of b; the smaller the value of b, the larger is the ratio β_r/β_1 for a given duration of deformation. The ratio, β_r/β_1, also increases with increasing tension ($\Delta p R_p/\mu$), which is consistent with the experimental observations of Chien et al. (4).

The time constant, β_r, predicted by the present model for the case of perfect adhesion after time $\tilde{t}_0 = 10$ is compared with experimental results in Fig. 8. This figure shows β_r as a function of the duration, $\tilde{t}_0$, of the deformation phase. The experimental points in the graph were obtained by

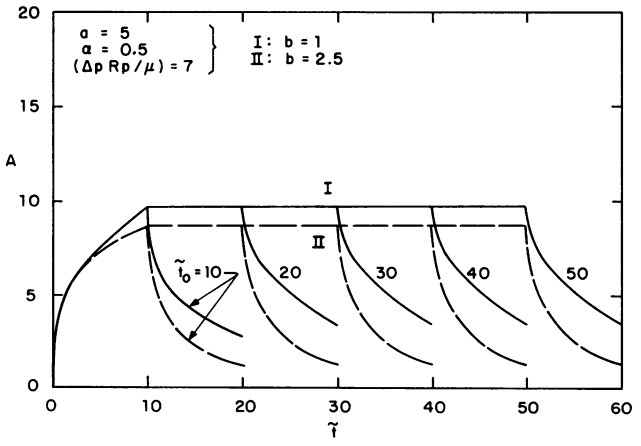

FIGURE 7 Dimensionless surface area A as a function of time $\tilde{t}$ for the case of complete adhesion when $\tilde{t}_0 > 10$.

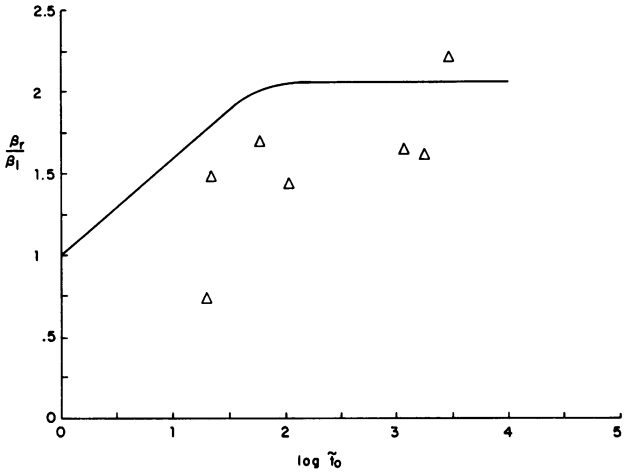

FIGURE 8 Variation of the time constant β_r with the duration of the deformation phase. (D_{pm}/R_p = 2.3, discrete points are experimental results, continuous curve is the prediction of the present model.)

using a single pipette, and the same pressure difference applied for different lengths of time. The figure indicates that the membrane model with a finite b value satisfactorily models the dependence of β_r on t_0 observed in the recovery phase of the experiments.

ANALYSIS OF THE TANK TREADING MOTION

It has been shown that erythrocytes suspended in a shear flow assume stationary shapes and orientation while the membrane rotates steadily around the cell (10). The time course of the orientation changes of the cell was considered by Keller and Skalak (11) by assuming the cell to be a triaxial ellipsoid. In the analysis, constitutive equations for the erythrocyte membrane were not taken into account, and the detailed analysis of the membrane stresses and strains was not considered. More recently, the details of the flow field external to the cell were investigated by Sutera and Tran-Son-Tay (12) under the same assumptions.

Similarly, erythrocytes observed to assume asymmetric shapes during flow through narrow capillaries (13) are considered to be associated with the tank-treading motion of the membrane. Recently, a two-dimensional model of the capillary flow of asymmetric red blood cells was introduced by Secomb and Skalak (14). This study does not attempt to compute the stresses and strains in the membrane exactly. More accurate models of the tank-treading motion of the erythrocytes in either infinite shear flow or flow through narrow capillaries would involve the solution of Stokes' equations inside and outside the cell coupled with the thin-shell equations of the erythrocyte membrane undergoing large deformations. The analysis is complicated further by the three-dimensional nature of the problem.

The discussion presented below considers a small planar segment of an erythrocyte membrane that undergoes

deformation which is quantitatively similar to that occurring in the tank-treading motion. Consider a rectangular segment of the membrane with initial coordinates in the domain $(0 < x_1 < x_1^0, 0 < x_2 < x_2^0)$. It is assumed that this segment is stretched at first to model the mean deformation observed in the tank-treading motion of the cell. For simplicitly, the mean stretch ratio λ_0 is considered to be a constant in the analysis. An additional deformation in the form of an oscillatory motion about the mean is superimposed to model the isochoric motion:

$$y_1 = \lambda_0 x_1(1 + e \sin 2\omega t) \tag{21}$$

$$y_2 = x_2/[\lambda_0(1 + e \sin 2\omega t)] \tag{22}$$

where x_i, y_i are as defined for Eq. 1, e is the amplitude of the oscillatory deformation, and ω is the frequency of the motion. The extension ratio λ in the x_1 direction and the rate of strain $(\dot{\lambda}/\lambda)$ corresponding to Eq. 12 can be written as

$$\lambda = (1 + e \sin 2\omega t)\, \lambda_0 \tag{23}$$

$$(\dot{\lambda}/\lambda) = (2e\omega \cos 2\omega t)/(1 + e \sin 2\omega t). \tag{24}$$

We now consider the rate equation (Eq. 9) applied to this deformation,

$$(l^2 - l^{-2}) = 4a\tau^* \left(\frac{\dot{\lambda}}{\lambda} - \frac{\dot{l}}{l}\right) + b\left(\frac{\lambda^2}{l^2} - \frac{l^2}{\lambda^2}\right) \tag{25}$$

with the initial conditions corresponding to a sudden start from rest:

$$l(0) = \lambda(0). \tag{26}$$

Numerical solutions of Eq. 25 indicate that if b is set equal to zero, the initial deformation λ_0 does not affect the values of l and the stress components $T_1 - T_0$, $T_2 - T_0$ after a transition period. The duration of the transition increases with an increasing value of a. Figs. 9 and 10 show the variation of the stress component $T_1 - T_0 = \mu[(l^2 - l^{-2}) + \tau^* \dot{\lambda}/\lambda]$ with respect to time, $\tilde{t}$, for $\lambda_0 = 1.0, 1.5, 2.0$, $b = 0$, 2, $a = 50$, and $\omega = 1$. It can also be shown that as ω increases the elastic stress T_1^e decreases and viscous stress T_1^v increases. In tank-treading motion, the frequency ω generally increases with an increasing applied strain rate on the cell. The present model also shows that the elastic strains caused by the deformation into a stationary shape decrease gradually with time. In the case of a fluid membrane ($b = 0$) the long term viscosity coefficient strongly influences the magnitude of the elastic strains that occur during tank treading. However, the membrane model with a finite b value will always have some residual elastic component depending on the magnitude of initial stretch. Hence, the model leads to an "elastic" length dependence on shear stress, which is consistent with the various shapes observed in tank-treading motion. As the frequency of tank-treading increases, the strain rate increases while the elastic strain remains bounded, and the viscous term governed by the membrane viscosity η becomes more dominant than the elastic stresses. Fischer and Schmid-Schönbein (10) predicts an essentially viscous membrane behavior of the erythrocyte membrane in tank-treading motion in a shear flow field. The results of the present model are consistent with his observations.

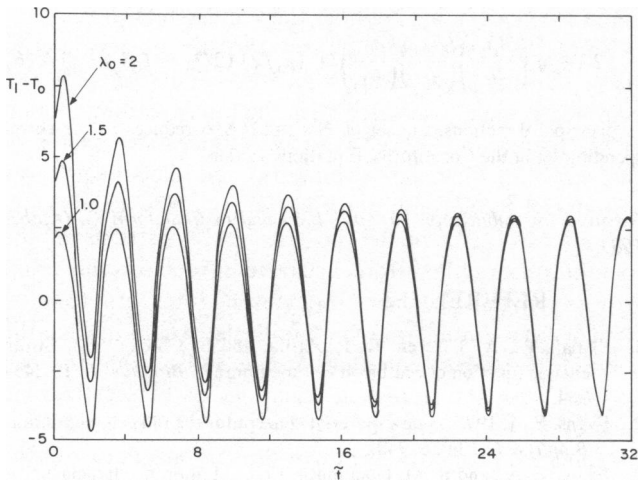

FIGURE 9 The stress component $(T_1 - T_0)$ as a function of time $\tilde{t}$ for the plane deformation given by Eq. 23 with $b = 0$, $a = 50$.

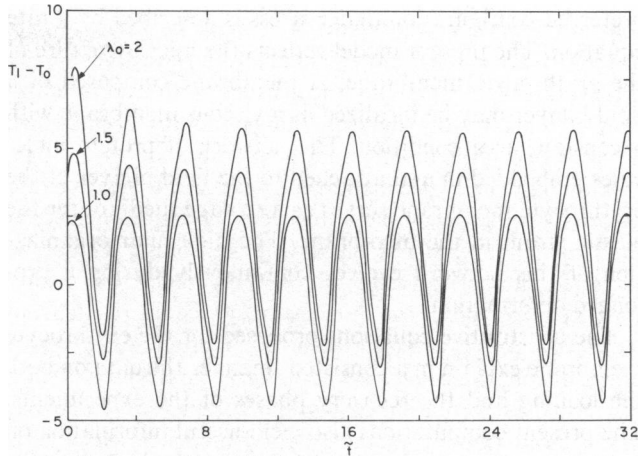

FIGURE 10 The stress component $(T_1 - T_0)$ as a function of time $\tilde{t}$ for the plane deformation given by Eq. 23 with $b = 2$, $a = 50$.

CONCLUSIONS

A nonlinear, two-dimensional constitutive equation was developed to model the viscoelastic properties of the erythrocyte membrane. The membrane tensions T_1, T_2 were assumed to be composed of three distinct terms. The first term is the isotropic tension due to the constant area stipulation. The second term represents viscous stresses with a viscosity coefficient that decreases with increasing rate of strain. The third term is due to the elastic strains, which are measured from the preferred configuration that evolves with time during deformation. The evolution of the

preferred configuration under stress is described by a rate equation. The present model reflects the microstructure of the erythrocyte membrane. A membrane composed of a lipid bilayer may be idealized as a viscous membrane with a constant area condition. The network of protein molecules embedded in and attached to the lipid bilayer of the erythrocyte membrane serves as a storage medium for the elastic strain in the membrane. The molecular organization of this network evolves continuously during a prolonged deformation.

The constitutive equations proposed for the erythrocyte membrane explain in a consistent manner the data on both the loading and the recovery phases of the experiments. The present computations also yield useful information on how the membrane viscosity becomes a dominant feature in tank-treading motion of erythrocytes in shear flow.

APPENDIX

Let (x_1, x_2) and (y_1, y_2) be initial and current material element coordinates, respectively. It is convenient to write the constitutive equation of a fluid membrane in the current state. Let the stress tensor T_{ij} in the instantaneous configuration be written as

$$T_{ij} = T_0\delta_{ij} + 2\eta D_{ij} + T^e_{ij} \tag{A1}$$

where T_0 is an isotropic tension. The rate of deformation tensor is defined as

$$D_{ij} = (1/2)\,(L_{ij} + L_{ji}) \tag{A2}$$

where L_{ij} is the spatial gradient of velocity V_i:

$$L_{ij} = \partial V_i/\partial y_j. \tag{A3}$$

The viscosity coefficient η has the shear thinning behavior described by the following equation:

$$\eta = \mu\tau^*/(1 + \tau' I_D) \tag{A4}$$

where

$$I^2_D = -\,det(D_{ij}). \tag{A5}$$

In the present analysis, elastic stress T^e_{ij} is assumed to be of the form

$$T^e_{ij} = 2\rho\frac{\partial W}{\partial I_c}\left(C_{ij} - \frac{1}{2}I_c\delta_{ij}\right). \tag{A6}$$

In this equation C_{ij} is a symmetric second-order tensor, I_C = trace (C_{ij}) is an invariant elastic strain in the protein network, ρ is the mass density per unit area in the current state, and W is the specific free energy per unit mass.

In the present analysis, it is assumed that the free energy W can be written as

$$W = (\mu/2\rho)\,(I_c - 2). \tag{A7}$$

Substitution of Eq. A7 into Eq. A6 yields

$$T^e_{ij} = \mu[C_{ij} - (1/2)I_C\delta_{ij}]. \tag{A8a}$$

In principal directions, this equation reduces to

$$T^e_{11} = (\mu/2)(l^2_1 - l^2_2), \qquad T^e_{22} = (\mu/2)(l^2_2 - l^2_1). \tag{A8b}$$

To complete the constitutive equations of the membrane model, a rate equation which accounts for the evolution of the protein network must be introduced. Let the upper convective derivative, $\hat{C}_{ij}$, be defined as (8):

$$\hat{C}_{ij} = C_{ij} + C_{ip}L_{pj} + L_{pi}C_{pj}. \tag{A9}$$

Consider the following evolution equation

$$\hat{C}_{ij} = C_{ip}T^e_{pj}/\eta_1$$

where η_1 is a constant. In principal directions, this equation reduces to Eq. 9 of the manuscript with $\mu_1 = 0$.

In the case of the solid membrane model with finite b, it will be more convenient to develop the equations in the undeformed configuration.

The Finger's strain tensor in classical elasticity is defined as

$$B_{ij} = \delta_{kl}\frac{\partial y_i}{\partial x_k}\frac{\partial y_j}{\partial x_l}. \tag{A10}$$

Let (dz_i, dz_j) be an infinitesimal line element in the preferred configuration, and assume that $[(\partial z_i/\partial x_j)]$ is defined at each point in the membrane. Let the strain tensor of the preferred configuration be defined as

$$Q_{ij} = \delta_{kl}\frac{\partial z_i}{\partial x_k}\frac{\partial z_j}{\partial x_l} \tag{A11}$$

and let $\bar{B}_{ij}$ be the elastic strain tensor in the protein network:

$$\bar{B}_{ij} = \delta_{kl}\frac{\partial y_i}{\partial z_k}\frac{\partial y_j}{\partial z_l}. \tag{A12}$$

The constitutive equation for the stress tensor, T_{ij}, can be written

$$T_{ij} = T\,\delta_{ij} + 2\eta D_{ij} + (\mu/2)(2\bar{B}_{ij} - I_B\,\delta_{ij}) \tag{A13}$$

where

$$I_{\bar{B}} = \text{trace}\,(\bar{B}_{ij}) \tag{A14}$$

and

$$D_{ij} = (1/2)\left(\frac{\partial B_{pq}}{\partial t}\right)\left(\frac{\partial x_p}{\partial y_i}\frac{\partial x_q}{\partial y_j}\right) \tag{A15}$$

is the rate of strain.

The following rate-of-evolution equation is assumed

$$T^e_{ij} = \eta_1\left(\frac{\partial Q_{pq}}{\partial t}\right)\left(\frac{\partial x_p}{\partial y_i}\right)\left(\frac{\partial x_q}{\partial y_j}\right) + (\mu_1/2)\,(2Q_{ij} - I_Q\delta_{ij}). \tag{A16}$$

In principal directions, the set of Eqs. A12–A16 reduces to the corresponding set in the Constitutive Equations section.

Received for publication 20 April 1983 and in final form 11 October 1983.

REFERENCES

1. Skalak, R., A. Tözeren, R. P. Zarda, and S. Chien. 1973. Strain energy function of red blood cell membranes. *Biophys. J.* 13:245–264.
2. Evans, E. A. 1973. A new material concept for the red cell membrane. *Biophys. J.* 13:926–940.
3. Evans, E. A., and R. M. Hochmuth. 1976. Membrane viscoelasticity. *Biophys. J.* 16:1–11.
4. Chien, S., K. L. P. Sung, R. Skalak, S. Usami, and A. Tözeren. 1978.

Theoretical and experimental studies on viscoelastic properties of erythrocyte membrane. *Biophys. J.* 24:463–487.

5. Tözeren, A., R. Skalak, K. L. P. Sung, and S. Chien. 1982. Viscoelastic behavior of erythrocyte membrane. *Biophys. J.* 39:23–32.
6. Bird, R. B., R. C. Armstrong, and O. Hassager. 1977. Dynamics of Polymeric Liquids. John Wiley & Sons, New York. 1:298–300.
7. Evans, E. A., and R. Skalak. 1980. Mechanics and thermodynamics of biomembranes. CRC Press, Boca Raton, FL. 129–141.
8. Dashner, P. A., and W. E. Vanarsdale. 1981. A phenomenological theory for elastic fluids. *J. Non-Newtonian Fluid Mech.* 8:59–67.
9. Lux, S. E. 1979. Dissecting the red cell membrane skeleton. *Nature (Lond.)*. 281:426–429.
10. Fischer, T. M., and H. Schmid-Schönbein. 1977. Tank tread motion of red cell membranes in viscometric flow: behavior of intracellular and extracellular markers (with film). *Blood Cells.* 3:351–365.
11. Keller, S. R., and R. Skalak. 1982. Motion of a tank-treading ellipsoidal particle in a shear flow. *J. Fluid Mech.* 120:27–47.
12. Sutera, S. P., and R. Tran-Son-Tay. 1982. Mathematical model of velocity field external to tank-treading red cell. Third International Conference Mechanics in Medicine and Biology. Universite de Technologie de Compiegne, France. 61–62.
13. Gaehtgens, P. 19 . In vitro studies of blood rheology in microscopic tubes. *In* The Rheology of Blood, Blood Vessels, and Associated Tissues. D. R. Gross and N. H. C. Hwang, editors. Sijthoff en Noordhoff International Publishers, Alphen aan den Rijn, The Netherlands. 257–275.
14. Secomb, T. W., and R. Skalak. 1982. A two-dimensional model for capillary flow of an asymmetric cell. *Microvasc. Research.* 24:194–203.